

# TiO<sub>2</sub>/Ag<sub>2</sub>O-Exfoliated Graphite as Visible Light-Responsive Nanostructure for Improved Photoelectrochemical Degradation of BPA

Onoyivwe Monday Ama<sup>1,3,\*</sup>, Khotso Khoele<sup>2,3</sup> and Suprakas Sinha Ray<sup>1,3</sup>

<sup>1</sup>Department of Applied Chemistry, University of Johannesburg,  
Doornfontein, 2028, Johannesburg, South Africa

<sup>2</sup>Tshwane University of Technology, Department of Chemical, Metallurgical and Materials  
Engineering, Pretoria, South Africa

<sup>3</sup>DST-CSIR National Center for Nanostructured Materials, Council for Scientific and  
Industrial Research, Pretoria 0001, South Africa

(\*) Corresponding author: onoyivwe4real@gmail.com  
(Received: 04 February 2019 and Accepted: 31 May 2020)

## Abstract

*In this paper, exfoliated graphite (EG), titanium dioxide (TiO<sub>2</sub>), silver oxide (Ag<sub>2</sub>O) and TiO<sub>2</sub>-Ag<sub>2</sub>O/EG have synthesized, fabricated and characterized. An electrolyte used in this work was Bisphenol A (BPA). Degradation was carried out under electrochemical oxidation, photolysis and photoelectrochemical. Characterization techniques utilized were: ultraviolet-visible (UV) diffuse reflectance analysis, scanning electron microscopy (SEM), energy dispersive spectroscopy (EDX), Raman, thermal gravimetric analyzer (TGA), and X-ray diffractometry (XRD). SEM morphologies, EDX and the XRD patterns showed a good mix and disperse among nanocomposites in terms of the formation of TiO<sub>2</sub>-Ag<sub>2</sub>O/EG. Degradation analysis revealed TiO<sub>2</sub>-Ag<sub>2</sub>O/EG as the best nanocomposite for degradation of azo dyes from the wastewater. On a relative view of engaged techniques, photoelectrochemical revealed to be worthwhile.*

**Keywords:** Ag<sub>2</sub>O, TiO<sub>2</sub>, Graphite, Bisphenol and photoelectrochemical.

## 1. INTRODUCTION

The development of clean and safe water is regarded as key to sustainability of life. Currently, the world is faced with a mounting challenge in saving the few available sources of “clean” water due to pollution. Continuous pollution has led to an increase in the rate of deteriorating water quality. Rapid industrialization has led to high discharge of persistent organic pollutants into the environment, causing serious damage to aquatic life as well as human well-being [1]. Among the pollutants causing deterioration in water quality are a unique class of compounds known as emerging pollutants. Bisphenol A (BPA), a synthetic organic compound which is widely used in several applications, for example, has been reported to act as an endocrine disruptor

[2, 3]. It can enter the aquatic system through industrial wastewater discharge or leaching from the products. BPA has a wide range of industrial applications, including, its utilization as a raw material for the manufacture of pesticides, polycarbonate and epoxy resins [1]. It is also utilized in the manufacture of flame retardants, plastic products, toys, medical equipment, and tubing. It has been reported to mimic or oppose the biological functions of natural hormones [4].

Hitherto, various methods have been proposed for the removal of BPA from wastewater. These include adsorption, biological treatment, chemical oxidation and advanced oxidation processes. However, advanced oxidation processes have been widely reported as potential

procedure to remove persistent organic pollutants, including, BPA from aqueous medium [5, 6]. Further, electrochemical advanced oxidation techniques have established themselves as efficient approaches for the decontamination of organic pollutants-containing wastewater, owing to their high efficiency as well as environmental compatibility [2]. The efficacy of these procedures are attributed to the formation of highly reactive species such as hydroxyl radical ( $\bullet\text{OH}$ ) with high redox potential that can mineralize organic pollutants [7].

$\text{TiO}_2$  is one of the most employed catalysts reported in literature for wastewater treatment. However, its practical application has been hindered by a number of challenges, including, high recombination rate of the photogenerated electron-hole pairs. In addition, this catalyst exhibits a wide band gap of 3.2 eV which restricts its application to UV light. To alleviate these challenges, combination with semiconductor possessing strong visible-light absorptivity owing to reduced band gap has been reported [8-14].  $\text{Ag}_2\text{O}$  is an attractive and good visible-light responsive semiconductor that has previously been reported to exhibit synergetic effect on nitrogen doped  $\text{TiO}_2$  for superior catalytic degradation of organic pollutant [15].

Photoelectrochemical procedure, known as the combination of photocatalysis and electrochemical oxidation technique has proven to be a rapid and highly efficient approach for organic pollutants degradation [9, 16, 17]. Exfoliated graphite on the other hand, has broadly been also reported as promising support for photoelectrochemical application owing to its electrical conductivities, large surface area, flexibility, corrosion resistance and enhanced [18-20].

The current investigation describes the preparation and evaluation of  $\text{TiO}_2/\text{Ag}_2\text{O}$ @EG electrode for electrocatalytic degradation of toxic BPA in aqueous environment under sunlight irradiation.

Moreover, a plausible mechanism for BPA degradation was anticipated through high performance liquid chromatography (HPLC) technique.

## **2. MATERIALS AND METHODS**

### **2.1. Synthesis of Rod-Like $\text{TiO}_2$**

$\text{TiO}_2$  nanoparticles were synthesized using a hydrothermal process. In a typical preparation procedure, 5 mL of titanium (IV) isopropoxide was dissolved in 10 mL of a mixture isopropyl alcohol/water (5:3). 10 mL of 15 M NaOH aqueous solution was then added and the mixture was stirred at room temperature for 3 h. Next, the reaction was transferred to a Teflon-lined autoclave and heated to 180 °C for 24 h before being allowed to naturally cool to room temperature. The product was washed several times with ethanol and distilled water until pH 7. In the end, the wet precipitate was dried in an oven at 60 °C and calcined at 500 °C in a muffle furnace in air.

### **2.2. Synthesis of $\text{TiO}_2/\text{Ag}_2\text{O}$**

0.64 g of  $\text{AgNO}_3$  and 0.3 g of  $\text{TiO}_2$  nanorod were mixed in 20 mL ethylene glycol. The solution mixture was sonicated for 30 min for good dispersion purpose. Then 0.1 M NaOH solutions were added dropwise so as to modify the pH value to 13, and stirred for 2 h. The product was isolated by filtration, washed many times using deionized water, and ultimately dried at 60 °C for 12 h.

### **2.3. Synthesis of EG**

As based on literature, 150 mg of EG was compressed to form EG pellet of 1 cm diameter, and one end of a coiled Cu wire using a glass tube with conducting silver paint was attached to a small size of the prepared EG pellet and was covered with epoxy resin [21].

### **2.4. Characterization**

For a proper observation on barely synthesized semiconductors and modified nanocomposites in terms of their

structures, phases and crystallinities present within them, X-Ray powder diffraction (XRD) was utilized. The engaged software was Philips PAN Analytical X'Pert System. The operational settings were voltage of 40 kV, 40 mA current and Cu-K $\alpha$  radiation of the 0.154 nm. The record of diffraction data started from 4° to 80° (step size: 0.02°, step time: 1min) at the normal 2 $\theta$  angles which is mostly utilized on XRD measurements. For the surface morphologies and elemental compositions of the samples, scanning electron microscopy (SEM) coupled to energy dispersive X-Ray (EDX) operating at 20 kV electron acceleration voltage was applied. A relative absorbance of the light on engaged nanocomposites was carried out using Shimadzu UV-2450, UV-vis spectrophotometer in the range of 200-800 nm. The micro-Raman spectrometer (NRS-3100) with a 532 nm solid-state primary laser as an excitation source in the backscattering configuration at room temperature was furthermore involved on matching JCPDS standard files peak positions, and also on recording of the phonon vibrational study of the different nanostructures and nanocomposites.

### 2.5. Degradation Experiments

In comparison of degradation efficiency from the techniques applied photolysis, electrochemical oxidation and photoelectrochemical curves were drawn up. For these experiments, a potentiostat/galvanostat operated at a voltage range between 2 V-5 V and a corresponding current range of 1mA-15mA was applied on degradation of the dye in 0.1 M sodium sulphate as a complementary electrode. Besides fabricated photoanode as working electrodes, two other electrodes were generally engaged: Ag/AgCl (3.0 M KCl) as a reference electrode and a platinum foil as a counter electrode. Pertinent surfaces of utilized photoanode were aligned to receive the beam of light directly from the solar simulator. Overall, an electro-

chemical cell was used to carry out all degradation experiments containing the photoanode and the BPA. Under solo-photolysis and electrochemical oxidation, light was applied for photolysis, while potential without solar simulation was applied for electrochemical oxidation. On synergistic photoelectrochemical degradation, potential and light were applied to the cell. Within that setup, a distance between the New Port 9600 Full Spectrum solar simulator equipped with 400 W and the experimental was measured at a distance of 10 cm, to study the degradation and the degradation kinetics of the BPA. The beam power was equivalent to 1 sun. Aliquots (5 ml) of the suspension were withdrawn using a disposable syringe and filtered through 0.4  $\mu$ m PVDF membrane filter at 10 min intervals for about 1 h. For the determination of supernatant solution, Shimadzu UV-2450 spectrophotometer of the concentration of methylene blue dye remaining after degradation. The aforementioned techniques were then used to investigate the degraded dye.

## 3. RESULT AND DISCUSSIONS

### 3.1 SEM Analysis

SEM surface morphologies shown in Fig. 2 reveal each concerned solo nanocomposite and the corresponding synergistic nanocomposite synthesized in this study. In Fig. 2(a), EG is characterized by an absolute well-arranged plane of graphite, while porous TiO<sub>2</sub> morphology can be observed in Fig. 2(b). With an exhibition of a regular spherical morphology an existence of the Ag<sub>2</sub>O was noted as can be seen in Fig. 2(c). Overall, a synergistic nanocomposite is shown in Fig. 2(d). There, all engaged solo nanocomposite morphologies can be seen in a mixed structure. This is evidenced by the EDX spectrum with: C for EG, Ti from TiO<sub>2</sub>, Ag from Ag<sub>2</sub>O and the O from obvious three nanocomposites. As these elements are therein from singular nanocomposite, this shows successful

synthesis of  $\text{TiO}_2\text{-Ag}_2\text{O/EG}$  from singular

nanocomposite [17, 22].

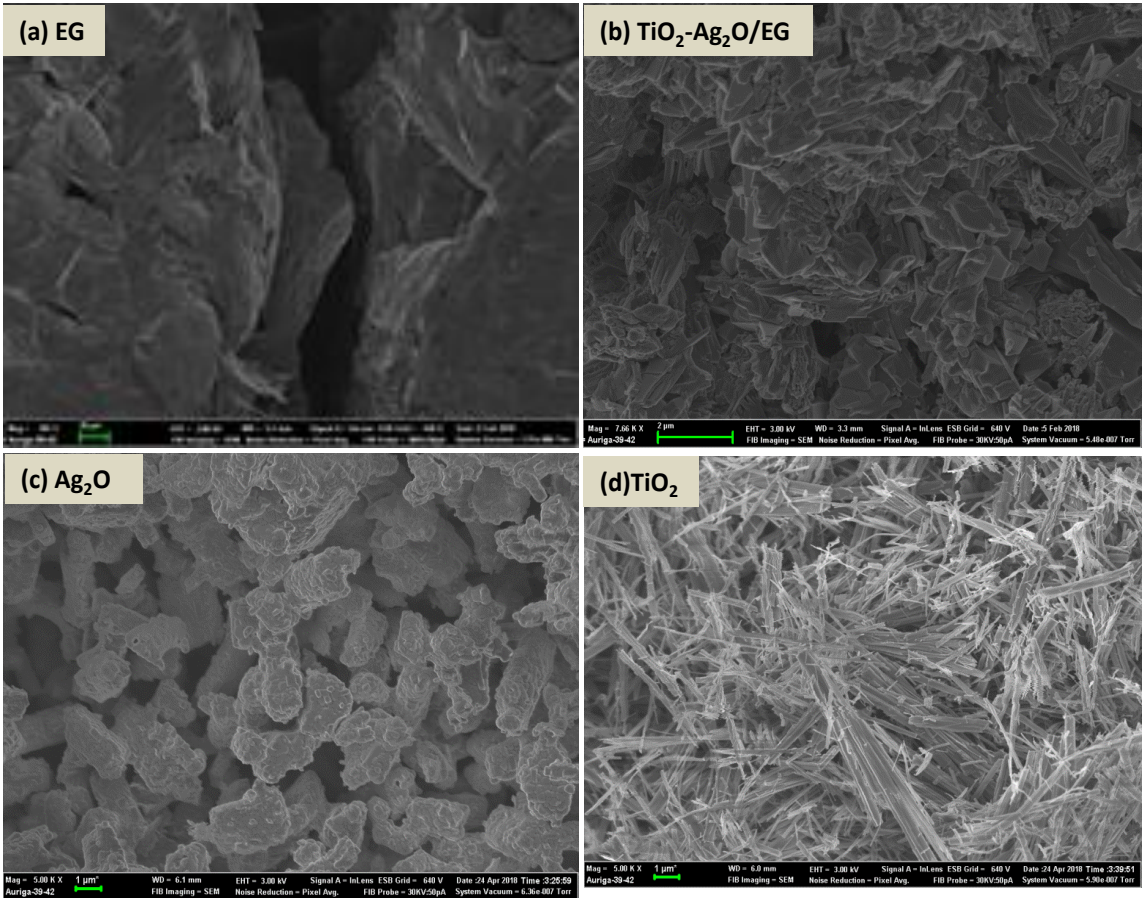
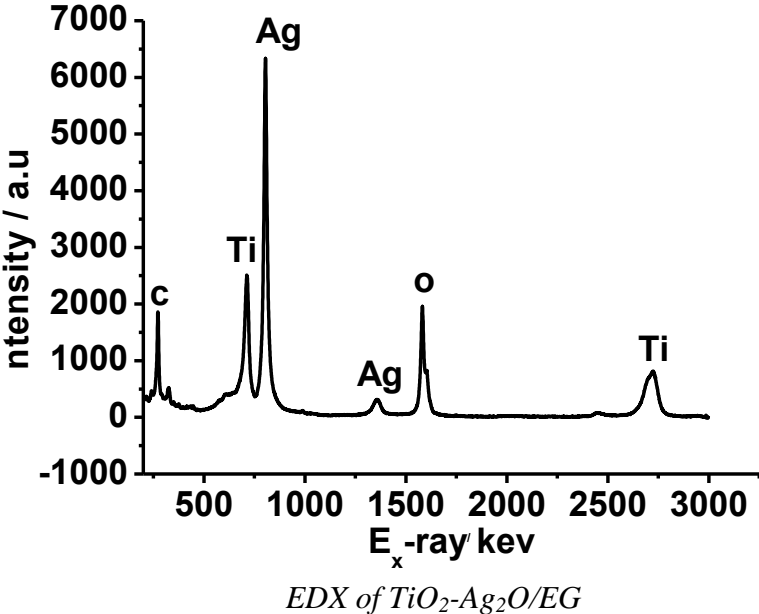
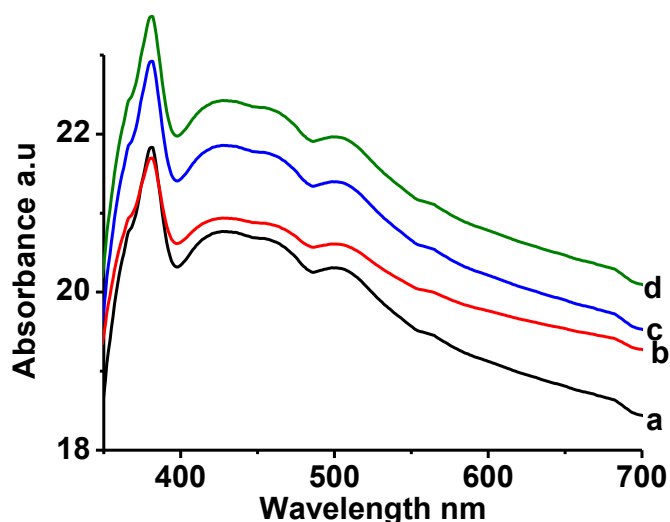


Figure 1. SEM Image of (a) EG (b)  $\text{TiO}_2\text{-Ag}_2\text{O/EG}$  (c)  $\text{Ag}_2\text{O}$  (d)  $\text{TiO}_2$ .





**Figure 2.** UV-Vis Absorbance Spectra of (a) EG (b) Ag<sub>2</sub>O (c) TiO<sub>2</sub> (d) TiO<sub>2</sub>-Ag<sub>2</sub>O/EG.

Fig. 3 shows a comparative XRD patterns of engaged nanocomposites in this study. This was particularly for the characterization of the structure, phase and crystallinity from singular nanocomposite to the modified synergistic nanocomposite: The engaged nanocomposites were as follows: a) EG, (b) Ag<sub>2</sub>O (c) TiO<sub>2</sub> (d) TiO<sub>2</sub>-Ag<sub>2</sub>O/EG. The first pattern shows a known monoclinic structure of TiO<sub>2</sub>. A face centred cubic (FCC) and characteristics of lattice vibration can be seen in Fig. 3 (ii). On the vivid observation of the whole Figure, a shift on solo nanocomposite in comparison to the TiO<sub>2</sub>-Ag<sub>2</sub>O/EG sample can be seen. Firstly, AgO<sub>2</sub> first peak which appears around 25.2° shifted a bit to an increased peak, and that is attributed to the inclusion of EG [3].

EG involvement is also associated with the reduction of the intensity of photoactive nanocomposites, and that is significant on degradation of dyes [23]. Furthermore, all Ag<sub>2</sub>O peaks which are found at 2θ values of 32.5°, 37.6°, 55.0°, 65.0° and 68.5° oscillated to (111), (200), (220), (311) and (222) shifted to the higher values. For the calculation of average crystallite size for the TiO<sub>2</sub>-Ag<sub>2</sub>O/EG, the popular utilized equation from Debye-Scherrer's was applied. Details of the equation can be found elsewhere [24]. Moreover, a propensity broadening peak on Ag<sub>2</sub>O was reduced on the synergistic sample (TiO<sub>2</sub>-Ag<sub>2</sub>O/EG) as can be seen in Fig. 3(iii). All these show that all engaged nanocomposites were mixed and dispersed evenly well.

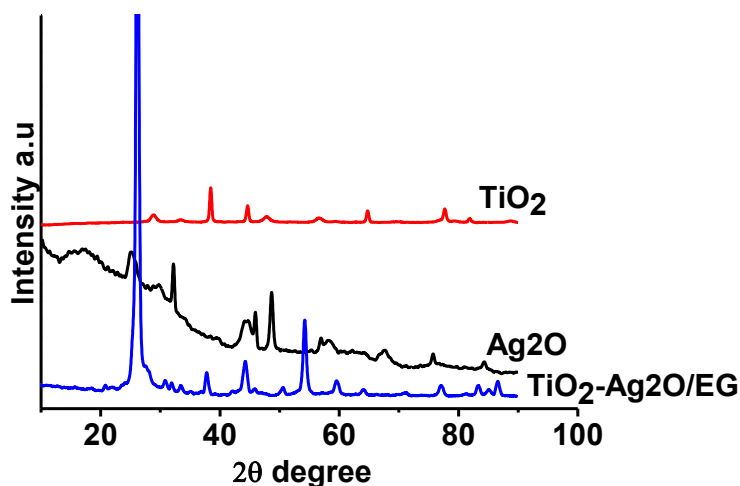


**Figure 3.** XRD Pattern of (b) Ag<sub>2</sub>O (c) TiO<sub>2</sub> (d) TiO<sub>2</sub>-Ag<sub>2</sub>O/EG.

On a further characterization of the modified TiO<sub>2</sub>-Ag<sub>2</sub>O/EG electrode for surface area and pore volume, BET surface analysis was conducted through nitrogen adsorption-desorption isotherm. As can be seen from Table 1, EG has both lowest surface area and pore volume, while TiO<sub>2</sub> has the highest surface area. On the other

hand, Ag<sub>2</sub>O has a pore volume higher than all three solo materials. Hence, a necessitation of improvement became paramount. Significantly, it can be seen that the surface area reduced to be in between of all the engaged solo-photoanodes, while the pore volume became highest.

**Table 1.** Show the BET result of (a) TiO<sub>2</sub>-Ag<sub>2</sub>O/EG (b) EG (c) TiO<sub>2</sub>-Ag<sub>2</sub>O.

Sample volume/cm <sup>3</sup> g g <sup>-1</sup>	BET surface area / m <sup>2</sup> g g <sup>-1</sup>	Pore
<b>EG</b>	11.98	. 0.0369
<b>TiO<sub>2</sub></b>	18.22	0.0452
<b>Ag<sub>2</sub>O</b>	12.31	0.6130
<b>TiO<sub>2</sub>-Ag<sub>2</sub>O/EG</b>	16.99	0.07996

Photoelectrochemical degradation of BPA Evaluation

### 3.2. Degradation Measurements

Fig. 3 shows UV curves obtained from UV spectrometer that was recorded within the wavelength range of 280-440 nm as function of absorbance of light. The operational setting were as follows: pH of 7 and 2.5 V potential. As can be seen in the figure, the removal of the BPA occurs as time goes by, and can particularly be observed between 280 and 320 nm. This observation is an indication that the TiO<sub>2</sub>-Ag<sub>2</sub>O/EG is an appropriate photoanode for effective photoelectrochemical degradation of BPA from the organic waste.

Synthesized EG, TiO<sub>2</sub>, Ag<sub>2</sub>O and TiO<sub>2</sub>-Ag<sub>2</sub>O/EG on degradation measurements are displayed in Fig. 4, while the Fig. 5 shows relative degradation efficiency of utilized techniques. Vividly, it can be seen that TiO<sub>2</sub>-Ag<sub>2</sub>O alone possesses low efficiency on degradation of the dye. However, an incorporation of the EG into the TiO<sub>2</sub>-Ag<sub>2</sub>O significantly improves degradation kinetics as can be seen in Fig.

4 (a). This is attributed to the magnificent properties of the EG with its structure with electrons trap sites [19]. Furthermore, the inclusion of TiO<sub>2</sub> within synergistic material is also attributed to a further generation of hydroxyl radicals which turns up with an excitation consists of photons with energy higher than or equal to its band gap, and thus leading to efficient degradation. Overall, degradation profile of the engaged techniques shown in Fig. 5, it can be seen that synergistic photoelectrochemical is worthwhile. Therefore, a combination of both photolysis and electrochemical oxidation is effective on removal of the azo dyes from the wastewater. The improved occurrence is associated to the limitations of photolysis which are covered by electrochemical oxidation and limitations of electrochemical oxidation. The details on both advantages and limitations of solo technique can be found elsewhere [25].

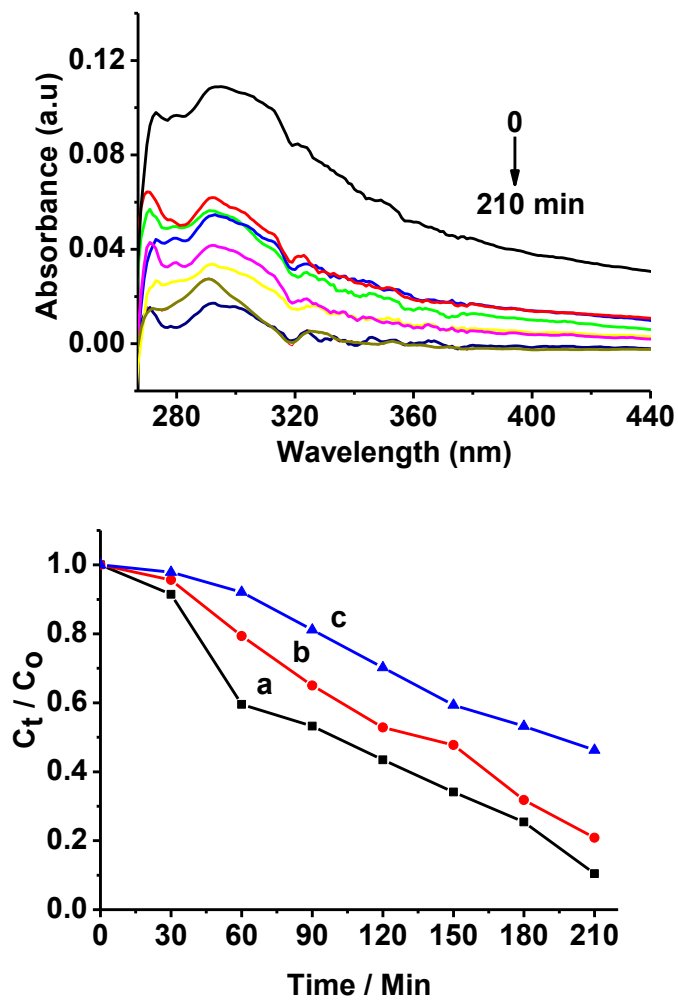


Figure 4. Degradation profile of (a)  $TiO_2-Ag_2O/EG$  (b)  $EG$  (c)  $TiO_2-Ag_2O$ .

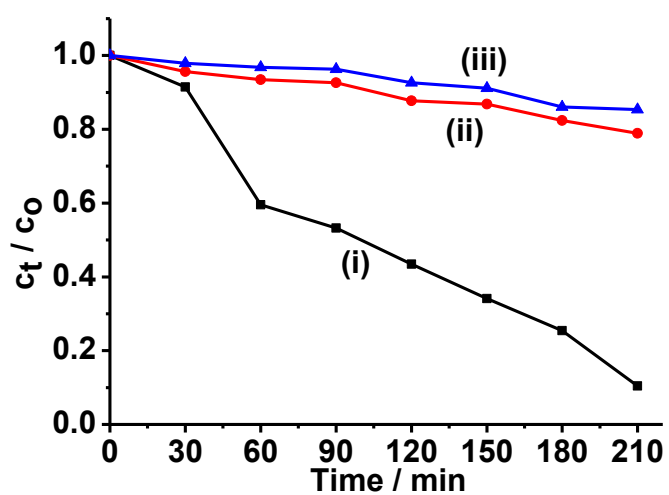
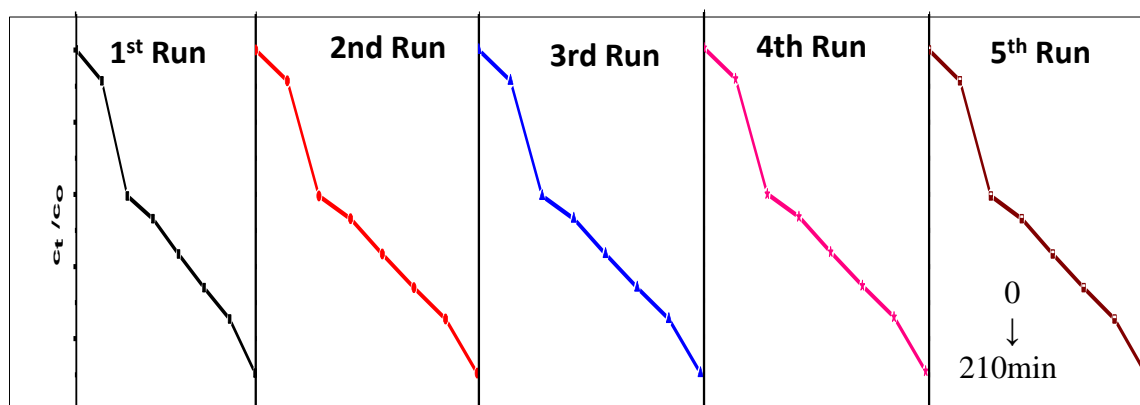


Figure 5. Degradation of (i) Photoelectrochemical (ii) Electrochemical oxidation (iii) Photolysis.

On characterization of probable multiple usage of  $\text{TiO}_2\text{-Ag}_2\text{O/EG}$  on photoelectrochemical degradation of dyes from wastewater, five consecutive cycles of photoelectrochemical degradation were run from 0 to 210 min. From the curves shown

in Fig. 6, the good photoelectrochemical re-usage can be observed. This occurrence is absolutely ideal for quasi-nil of secondary pollution, and this is efficient on the entire photoelectrochemical degradation utilization [12].



**Figure 6.** Five cycle degradation test of the  $\text{TiO}_2\text{-Ag}_2\text{O/EG}$  electrode for the photoelectrochemical degradation of (dye name).

Table 2 below compares semiconductors which consist EG in degradation of azo dyes from the wastewater. First, it can be seen from Table 2 that the presently fabricated  $\text{EG/TiO}_2\text{-Ag}_2\text{O}$  yields relatively good degradation efficiency. Second, on comparison which centres between bare

$\text{Ag}_2\text{O/TiO}_2$  on and  $\text{EG/TiO}_2\text{-Ag}_2\text{O}$ , it can vividly be seen that  $\text{Ag}_2\text{O/TiO}_2$  yielded 66% while  $\text{EG/TiO}_2\text{-Ag}_2\text{O}$  gave 87% degradation efficiency. This therefore suggests an incorporation of EG to the bare  $\text{Ag}_2\text{O/TiO}_2$  is more worthwhile on degradation of azo dyes from wastewater.

**Table 2.** Comparison of Catalysts used in Degradation of Exfoliated Graphite.

Used Catalysts Reference	Dyes Degradations	Efficiency
PD-ZnO-EG [26]	Acid Orange	87%
$\text{WO}_3/\text{EG}$ [27]	2-nitrophenol	82%
$\text{Ag}_2\text{O/TiO}_2$ [28]	Phenol	66%
EG/diamond [29]	Anthraquinone	81%
$\text{EG/TiO}_2\text{-Ag}_2\text{O}$ The current study	Bisphenol A	87%

#### 4. CONCLUSION

In this study, synthesis, fabrication and characterization of EG,  $\text{TiO}_2$  and  $\text{EG/}$

$\text{Ag}_2\text{O.TiO}_2$  were carried successfully. The following conclusions were overall drawn up from characterization techniques



applied on engaged solution and electrolytes:

- XRD revealed a propensity broadening peak on Ag<sub>2</sub>O to be reduced when it is mixed with EG and TiO<sub>2</sub>.
- The SEM image showed coordination of all singular nanocomposites in synergistic EG/Ag<sub>2</sub>O.TiO<sub>2</sub> nanocomposite.
- The EG/ MnO<sub>2</sub> exhibited improved visible light absorption compared to the singular nanocomposite, and that resulted to a higher Photoelectrochemical degradation efficiency.
- The photoelectrochemical method of degradation was observed to be more efficient than photolysis and photochemical oxidation methods on their solo application.
- The photoelectrochemical degradation method achieved 87% degradation efficiency within 240 min, and that underpins the fact that it is an appropriate electrode for the elimination of BPA dyes from the wastewater using EG/Ag<sub>2</sub>O.TiO<sub>2</sub> as the photo anode.

## REFERENCES

1. Hurwitz, G., Pornwongthong, P., Mahendra, S., Hoek, E. M., "Degradation of phenol by synergistic chlorine-enhanced photo-assisted electrochemical oxidation", *Chemical Engineering Journal*, 240 (2014) 235-243.
2. Cao, J., Xu, B., Lin, H., Luo, B., Chen, S., "Novel heterostructured Bi<sub>2</sub>S<sub>3</sub>/BiOI photocatalyst: facile preparation, characterization and visible light photocatalytic performance", *Dalton Transactions*, 41(37) (2012) 11482-11490.
3. Paul, K. K., Ghosh, R., Giri, P. K., "Mechanism of strong visible light photocatalysis by Ag<sub>2</sub>O-nanoparticle-decorated monoclinic TiO<sub>2</sub> (B) porous nanorods", *Nanotechnology*, 27(31) (2016) 315703.
4. Welshons, W. V., Nagel, S. C., vom Saal, F. S., "Large effects from small exposures. III. Endocrine mechanisms mediating effects of bisphenol A at levels of human exposure", *Endocrinology*, 147(6) (2006) s56-s69.
5. Malpass, G. R. P., Miwa, D. W., Miwa, A. C. P., Machado, S. A. S., Motheo, A. J., "Photo-assisted electrochemical oxidation of atrazine on a commercial Ti/Ru<sub>0.3</sub>Ti<sub>0.7</sub>O<sub>2</sub> DSA electrode", *Environmental Science & Technology*, 41(20) (2007) 7120-7125.
6. Zhao, X., Zhu, Y., "Synergetic degradation of rhodamine B at a porous ZnWO<sub>4</sub> film electrode by combined electro-oxidation and photocatalysis", *Environmental Science & Technology*, 40(10) (2006) 3367-3372.
7. Liu, J. J., Fu, X. L., Chen, S. F., Zhu, Y. F., "Electronic structure and optical properties of Ag<sub>3</sub>PO<sub>4</sub> photocatalyst calculated by hybrid density functional method", *Applied Physics Letters*, 99(19) (2011) 191903.
8. Vasilaki, E., Vamvakaki, M., Katsarakis, N., "Complex ZnO-TiO<sub>2</sub> core-shell flower-like architectures with enhanced photocatalytic performance and superhydrophilicity without UV irradiation", *Langmuir*, (2018).
9. Luo, J., Hepel, M., "Photoelectrochemical degradation of naphthol blue black diazo dye on WO<sub>3</sub> film electrode", *Electrochimica Acta*, 46(19) (2001) 2913-2922.
10. Gong, W., Meng, X., Tang, X., Ji, P., "Core-Shell MnO<sub>2</sub>-SiO<sub>2</sub> Nanorods for Catalyzing the Removal of Dyes from Water", *Catalysts*, 7(1) (2017) 19-23.
11. Chan, S. H. S., Yeong Wu, T., Juan, J. C., Teh, C. Y., "Recent developments of metal oxide semiconductors as photocatalysts in advanced oxidation processes (AOPs) for treatment of dye waste-water", *Journal of Chemical Technology & Biotechnology*, 86(9) (2011) 1130-1158.
12. Fu, S., He, Y., Wu, Q., Wu, Y., Wu, T., "Visible-light responsive plasmonic Ag<sub>2</sub>O/Ag/gC<sub>3</sub>N<sub>4</sub> nanosheets with enhanced photocatalytic degradation of Rhodamine B", *Journal of Materials Research*, 31(15) (2016) 2252-2260.
13. Kumar, P. S., Selvakumar, M., Babu, S. G., Induja, S., Karuthapandian, S., "CuO/ZnO nanorods: an affordable efficient pn heterojunction and morphology dependent photocatalytic activity against organic contaminants", *Journal of Alloys and Compounds*, 701 (2017) 562-573.
14. Sathishkumar, P., Sweena, R., Wu, J. J., Anandan, S., "Synthesis of CuO-ZnO nanophotocatalyst for visible light assisted degradation of a textile dye in aqueous solution", *Chemical Engineering Journal*, 171(1) (2011) 136-140.
15. Wang, C., Cai, X., Chen, Y., Cheng, Z., Luo, X., Mo, S., Sun, S., "Efficient hydrogen production from glycerol photoreforming over Ag<sub>2</sub>O/TiO<sub>2</sub> synthesized by a sol-gel method", *International Journal of Hydrogen Energy*, 42(27) (2017) 17063-17074.

16. An, T., Xiong, Y., Li, G., Zha, C., Zhu, X., "Synergetic effect in degradation of formic acid using a new photoelectrochemical reactor", *Journal of Photochemistry and Photobiology A: Chemistry*, 152(1-3) (2002) 155-165.
17. Asmussen, R. M., Tian, M., Chen, A., "A new approach to wastewater remediation based on bifunctional electrodes", *Environmental Science & Technology*, 43(13) (2009) 5100-5105.
18. Ama, O. M., "Synthesis, characterisation and photoelectrochemical studies of graphite/zinc oxide nanocomposites with the application exfoliated electrodes for the degradation of methylene blue" *Int. J. Nano Med. & Eng.*, 2(8) (2017) 145-151.
19. Ama, O. M., Kumar, N., Adams, F. V., Ray, S. S., "Efficient and cost-effective photoelectrochemical degradation of dyes in wastewater over an exfoliated graphite-MnO<sub>3</sub> nanocomposite electrode", *Electrocatalysis*, 63 (2018) 1-9.
20. Ama, O. M., Arotiba, O. A., "Exfoliated graphite/titanium dioxide for enhanced photoelectrochemical degradation of methylene blue dye under simulated visible light irradiation", *Journal of Electroanalytical Chemistry*, 803 (2017) 157-164.
21. Ama, O. M., Mabuba, N., Arotiba, O. A., "Synthesis, characterization, and application of exfoliated graphite/zirconium nanocomposite electrode for the photoelectrochemical degradation of organic dye in water", *Electrocatalysis*, 6(4) (2015) 390-397.
22. Ahmad, J., Majid, K., "In-situ synthesis of visible-light responsive Ag<sub>2</sub>O/graphene oxide nanocomposites and effect of graphene oxide content on its photocatalytic activity", *Advanced Composites and Hybrid Materials*, 61 (2018) 1-15.
23. Guo, Y., Peng, F., Wang, H., Huang, F., Meng, F., Hui, D., Zhou, Z., "Intercalation polymerization approach for preparing graphene/polymer composites", *Polymers*, 10(1) (2018) 61-68.
24. Sivaraj, D., Vijayalakshmi, K., "Preferential killing of bacterial cells by hybrid carbon nanotube-MnO<sub>2</sub> nanocomposite synthesized by novel microwave assisted processing", *Materials Science and Engineering: C*, 81 (2017) 469-477.
25. An, T. C., Zhu, X. H., Xiong, Y., "Feasibility study of photoelectrochemical degradation of methylene blue with three-dimensional electrode-photocatalytic reactor", *Chemosphere*, 46(6) (2002) 897-903.
26. Umukoro, E. H., Madyibi, S. S., Peleyeju, M. G., Tshwenya, L., Viljoen, E. H., Ngila, J. C., Arotiba, O. A. (2017). Photocatalytic application of Pd-ZnO-exfoliated graphite nanocomposite for the enhanced removal of acid orange 7 dye in water. *Solid State Sciences*, 74, 118-124.
27. Umukoro, E. H., Peleyeju, M. G., Ngila, J. C., Arotiba, O. A., "Towards wastewater treatment: Photo-assisted electrochemical degradation of 2-nitrophenol and orange II dye at a tungsten trioxide-exfoliated graphite composite electrode", *Chemical Engineering Journal*, 317 (2017) 290-301.
28. Jiang, B., Jiang, L., Shi, X., Wang, W., Li, G., Zhu, F., Zhang, D., "Ag<sub>2</sub>O/TiO<sub>2</sub> nanorods heterojunctions as a strong visible-light photocatalyst for phenol treatment", *Journal of Sol-Gel Science and Technology*, 73(2) (2015) 314-321.
29. Peleyeju, M. G., Umukoro, E. H., Babalola, J. O., Arotiba, O. A., "Electrochemical degradation of an anthraquinonic dye on an expanded graphite-diamond composite electrode", *Electrocatalysis*, 7(2) (2016) 132-139.